

## The spectral effects of clouds on solar irradiance

Jasmine S. Bartlett,<sup>1</sup> Áurea M. Ciotti, Richard F. Davis, and John J. Cullen

Center for Environmental Observation Technology and Research, Department of Oceanography  
Dalhousie University, Halifax, Nova Scotia, Canada

**Abstract.** Knowledge of the spectral attenuation associated with clouds is important for accurate estimates of natural irradiance at the Earth's surface. We compare spectral measurements of visible downwelling irradiance, under varying sky conditions at Halifax, Nova Scotia, Canada, with results from a clear-sky model. The spectral effect of clouds is estimated by taking the ratio of the measurements to the modeled irradiances and removing spectrally consistent instrumental effects and errors in the model. Empirical relationships derived between the spectral cloud effect and both  $CF$ , the cloud factor (the ratio of measured to modeled irradiances at 490 nm), and  $f$ , the fraction of sky covered by cloud, were found to follow a wavelength ( $\lambda$ ) dependence of the form  $a(CF \text{ or } f) + b(CF \text{ or } f)(\lambda/490)^{-4}$  in the 412–700 nm wavelength range. Both this relationship and a previously published linear relationship were found to be inadequate for describing cloudy irradiance data from the Bering Sea, indicating that the spectral effect of clouds can vary with cloud type and location. We show here that the spectral cloud effect can be mimicked by using a clear-sky model and changing the magnitude of the sky reflectivity or the spectral shape and magnitude of the ground albedo within the model. An investigation of the effects of cloud-dependent changes in irradiance spectra on calculations of bio-optical properties is also presented. Estimates of chlorophyll concentration from near-surface radiances are found to vary by up to 30%, whereas the effects on estimates of photosynthetically available and usable radiation at the sea surface are negligible.

### 1. Introduction

The accurate representation of natural spectral irradiance at the Earth's surface is an important factor in oceanographic studies based on optical measurements, such as the estimation of primary production [Kiefer and Mitchell, 1983; Platt and Sathyendranath, 1988; Morel, 1991] and chlorophyll concentration [Morel, 1980]. Although it is well known that clouds change the amount of sunlight reaching the Earth's surface, the spectral effect of clouds is poorly quantified. This uncertainty hampers attempts to model irradiance at the Earth's surface under natural atmospheric conditions.

Many models of solar irradiance apply to clear-sky conditions only [e.g., Leckner, 1978; Sherry and Justus, 1983; Bird and Riordan, 1986; Gregg and Carder, 1990; Gueymard, 1995]. Several methods have been used to incorporate the effect of clouds into such mod-

els. The more complicated representations divide the atmosphere and clouds into several layers, requiring numerous parameters (e.g., LOWTRAN [Kneizys *et al.*, 1983] and SBDART [Ricchiazzi *et al.*, 1998]). Simpler methods compensate for clouds by applying a weighting to the irradiance for the clear-sky case [e.g., Atwater and Ball, 1978]. A limited number of studies have shown that in the ultraviolet and visible wavelength regions (from 290 to 700 nm) clouds cause wavelength-dependent attenuation of downwelling solar irradiance [Spinhirne and Green, 1978; Nann, 1990; Nann and Riordan, 1991; Seckmeyer *et al.*, 1996; Wang and Lenoble, 1996; Byfield *et al.*, 1997; Siegel *et al.*, 1998]. Only the study of Siegel *et al.* [1998] provides a parameterization with coefficients that characterize the spectral effect of clouds on irradiance. However its applicability to a broad range of locations and times of year has not been determined.

Different perceptions exist regarding the cause of spectral attenuation by clouds. One hypothesis is that the spectral change in downwelling irradiance is a result of irradiance reflection off the surface of the Earth and clouds [Wang and Lenoble, 1996; Kylling *et al.*, 1997; Frederick, 1997; S. Madronich, personal communication, 1996]. The process is summarized as follows: Downwelling solar irradiance is reflected off the top sur-

<sup>1</sup>Now at the College of Oceanic and Atmospheric Sciences, Oregon State University, Corvallis.

face of clouds back to space. Since clouds are generally white or light gray in color, this process is spectrally neutral and simply decreases the magnitude of the downwelling irradiance. Part of this reflected irradiance is then scattered back toward the Earth's surface by the atmospheric constituents. The scattering is greater at shorter (blue) wavelengths than at longer (red) wavelengths, so the resulting downwelling irradiance is bluer relative to irradiance under clear sky. Downwelling irradiance that passes through the cloud and reaches the Earth's surface is then reflected (with a reflectivity determined by the ground albedo), yielding upwelling irradiance. Part of the upwelling irradiance is then reflected off the spectrally neutral bottom surface of the overlaying clouds, yielding downwelling irradiance which contributes to the direct downwelling irradiance. The spectral shape of this reflected downwelling irradiance would differ from that of the direct irradiance because of the influence of (a) the spectral shape of the ground albedo [Middleton, 1954; Spinhrne and Green, 1978] and (b) the spectral processes that occur within the atmospheric path traversed by the reflected irradiance that is not traversed by the direct irradiance.

An alternative hypothesis is that the spectral attenuation of clouds is caused by "spectral trapping" within the clouds: a consequence of the increase in pathlength caused by multiple scattering by the cloud constituents (water, gas molecules, and aerosols) which each have different absorption and scattering characteristics (but see Middleton [1954] and Spinhrne and Green [1978]). Our results suggest that the former hypothesis is the dominant effect in spectral attenuation by clouds.

Other factors that may alter the spectral shape of the downwelling irradiance under clouds are the cloud type, the solar zenith angle, and the horizontal cloud distribution. The spectral cloud effect has been shown to be enhanced under thick clouds relative to thin clouds [Spinhrne and Green, 1978]. However, the effect of an increase in solar zenith angle has only been seen during periods of thin cloud cover [Kasten and Czeplak, 1980; Nann and Riordan, 1991; Siegel et al., 1998]. This is because in thicker clouds the increased scattering by cloud particles causes the light field to become diffuse; hence the incident photon direction becomes irrelevant [Wang and Lenoble, 1996; Siegel et al., 1998]. An increase in the horizontal extent of cloud would also be expected to increase the spectral change in the downwelling irradiance because of the increasing number of photons that must intercept the cloud. However, the spectral cloud effect can be more pronounced when a small cloud is in the line-of-sight of the sun, since the direct downwelling irradiance will be intercepted by the cloud, whereas the skylight will be largely unaffected. This effect may be significant on short timescales when variations in downwelling irradiance caused by the passage of clouds in front of the sun can be severe [e.g., Cullen et al., 1994]. All of these factors need to be con-

sidered when determining the spectral effect of clouds.

This study determines the spectral effect that different sky conditions have on the visible irradiance at Halifax, Nova Scotia, Canada (45°N, 63°W), and derives simple methods to correct irradiance models for these spectral effects. The results are compared with previously published relationships and applied to irradiance data from the Bering Sea to determine the applicability of the derived results to other locations. A simple analysis is then made of the consequence of these spectral effects on the estimation of chlorophyll concentration ( $C$ ) in oceanic waters from measurements of ocean color at the sea surface and in the determination of photosynthetically available radiation (PAR) and photosynthetically usable radiation (PUR). A list of symbols and abbreviations can be found in the notation section.

## 2. Obtaining Cloudy Irradiance from Clear-Sky Irradiance

Downwelling solar irradiance after passing through cloud [ $E_d(\lambda, f)$ ] can be calculated from modeled clear-sky irradiance [ $\dot{E}_d(\lambda)$ ] as

$$E_d(\lambda, f) = \dot{E}_d(\lambda) \times X(\lambda) \times CF \times SCE(\lambda, CF), \quad (1)$$

where  $\lambda$  is the wavelength,  $f$  is the fraction of sky covered by cloud,  $X(\lambda)$  is the instrumental and/or local effect,  $CF$  is the cloud factor (the ratio of  $E_d(490)$  to  $\dot{E}_d(490)$ , a measure of the effect of clouds on the magnitude of the downwelling irradiance) and  $SCE(\lambda, CF)$  is the spectral cloud effect. The parameter  $X(\lambda)$  can be calculated for any instrument and location by taking the ratio of  $E_d(\lambda, 0)$  to  $\dot{E}_d(\lambda)$  using the available climatological parameters. The second parameter,  $CF$ , can be estimated by using a local parameterization for  $CF$  as a function of  $f$  or measured directly. The final parameter,  $SCE(\lambda, CF)$ , can either be calculated for a given locality or estimated from an empirical relationship. Each of these parameters are described in more detail later in this paper.

## 3. Irradiance Measurements

Measurements of spectral downwelling irradiance at the Earth's surface,  $E_d(\lambda)$ , were made using an OCI-200 irradiance meter (Satlantic, Inc., Halifax, Nova Scotia, Canada). This instrument has seven irradiance sensors with individual cosine collectors arranged in a horizontal plane; one sensor was not used because its cosine response was unsatisfactory. Each of the sensors used has a bandpass of approximately 10 nm [see Cullen et al., 1994], with center wavelengths of 411.4, 442.9, 489.9, 555.2, 683.8, and 699.5 nm. For these sensors, the errors in the cosine response for incident angles less than 70° were less than 7% (Figure 1). The spectral responses for the filters were determined at room temperature by Satlantic, Inc., using a dual-beam spec-

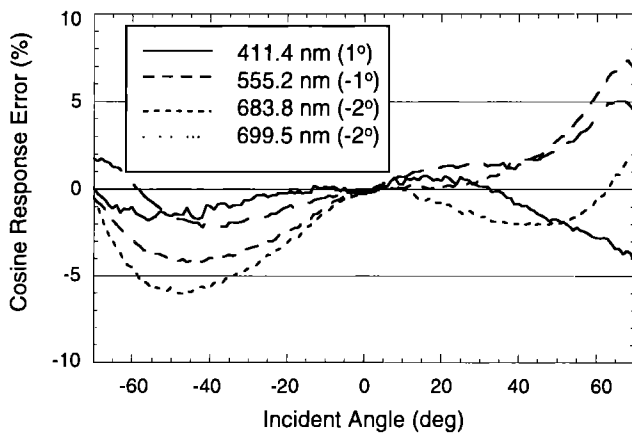


**Figure 1.** Cosine response errors for the OCI-200 irradiance sensors in air of center wavelengths 411.4, 555.2, 683.8, and 699.5 nm (courtesy of Satlantic, Inc.). The remaining sensors used (with center wavelengths of 442.9 and 489.9 nm) had cosine response errors of less than 5% for incident angles less than 70°. The values in parentheses indicate the angle of deviation of the instrument from the normal to the light source. These cosine response errors were determined in multiples of 2 or 3 by Satlantic, Inc., by varying the angle of incidence of a collimated light source on a row of sensors on an instrument head.

trophotometer with the filters positioned to mimic its location in the OCI-200 irradiance meter.

The instrument was positioned horizontally on the roof of an inner-city building in Halifax (population 125,000), 2 km from the ocean. Spectral irradiance was logged every 10 s for the months of August–October 1996. The instrument was calibrated each month using a standard 1000 W FEL Tungsten-Halogen lamp from Optronic Laboratories. Over the period of observation, the calibration values changed by a maximum of 4%.

#### 4. Modeled Clear-Sky Irradiance

Clear-sky irradiance at the Earth's surface was modeled using a combination of the original Bird and Riordan model designed for use on land [Bird and Riordan, 1986] and the modified version designed for use at sea [Gregg and Carder, 1990]. The main differences between these two versions are in the treatment of surface reflectance and aerosols, and the wavelength intervals that are used. The two versions were combined to produce a single model (the BRGC model (see Appendix)) for use between 300 and 700 nm either on land or at sea.

The model calculates clear-sky irradiance at the Earth's surface,  $\hat{E}_d(\lambda)$ , by attenuating extraterrestrial irradiance through the atmosphere and accounting for interaction with the surface. The magnitude and spectral characteristics of the attenuation are functions of the atmospheric constituents, the time of year, and the solar zenith angle. This study was performed with a

resolution of 1 nm using data of extraterrestrial irradiance and coefficients of absorption for ozone, oxygen, and water vapor from Gregg and Carder [1990] and K. Arrigo (personal communication, 1994). With the available climatological data (measured hourly), this model provides clear-sky irradiance at the Earth's surface with 1 nm resolution for every hour of the day.

The climatological data required by the model include ozone scale height, surface pressure, surface temperature, dew point temperature, visibility, windspeed, and 24-hour mean windspeed. Preliminary daily data of ozone scale height were obtained from the Bedford branch of Environment Canada (Bedford, Nova Scotia), which is located approximately 8 km from the site of our measurements. On days when no measurements of ozone were available, the mean value for the month was used. The remaining climatological variables were measured at least hourly approximately 6 km from the site of our measurements at Shearwater, Nova Scotia, by Environment Canada. When these observations were unavailable, the corresponding measurements of solar irradiance were not examined.

For the region under study, an air mass type of 2 was assumed (where a value of 1 applies to marine atmospheres, and 10 applies to urban atmospheres). The ground albedo was assumed to be spectrally neutral with a value of 0.2, which is assumed to be representative of the surrounding area. This is an average of typical values for soil, concrete, basalt, pinetrees, and grass in the visible wavelength region [Gueymard, 1995].

#### 5. Measurement-Model Comparison

By comparing the spectral shape of cloudy downwelling irradiance measured at the Earth's surface with the spectral shape of the corresponding modeled irradiance for clear-sky conditions, it should be possible to determine the spectral effect that clouds have on irradiance. However, this type of approach makes several assumptions: (1) that the measured and modeled irradiances are comparable in wavelength and temporal resolution, (2) that the model results are accurate for the locality, and (3) that any differences observed are solely a consequence of the presence of clouds and not of any other factors, such as poor approximations of aerosols or instrumental effects. An attempt will be made to minimize the effects of these assumptions.

The different resolution in wavelength between the model and the measurements is accounted for by multiplying the model spectra by the spectral response of the instrument at each waveband (normalized to have unit integrals). The different temporal resolutions are accounted for by comparing the model, based on hourly climatological observations, with measurements (made every 10 s) averaged over 10-min periods centered on the time of climatological data observation.

Comparison between the modeled and measured irradiances for three hours on a clear day (Figure 2) shows

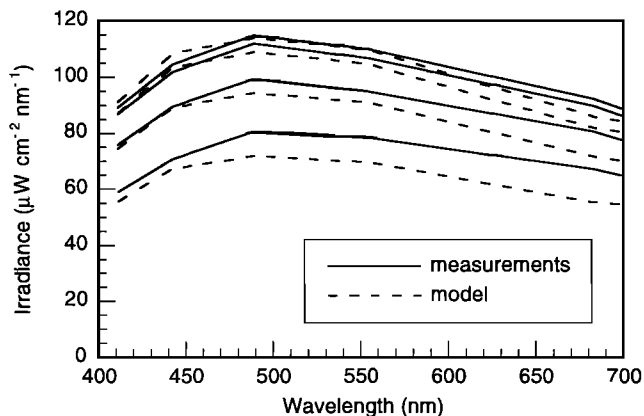


**Figure 2.** Comparison of irradiances measured under clear sky conditions (solid lines) with modeled clear-sky irradiances (dashed lines). The measured data shown are 10-min averages (centered on the hour) of measurements made on September 27, 1996, from 1000 to 1300 LT. The modeled lines shown are the result of combining the 1 nm resolution clear-sky model results with the spectral response of the instrument. See the text for details of the model.

that the general trends and magnitudes of the measured and modeled clear-sky irradiances agree, but there are consistent differences, particularly at 490 nm and from 683 to 700 nm. These differences could be due to either instrumental effects (i.e., deviations from the idealized response) or inability of the model to simulate accurately the local conditions because of the presence of pollution or the use of an inappropriate ground albedo, for example.

## 6. Estimation of the Spectral Effects of Clouds

To determine the spectral effect of clouds on irradiance, the ratios of each of the measured spectra to their corresponding modeled clear-sky spectra,  $E_d(\lambda)/\hat{E}_d(\lambda)$ , were calculated. Data were limited to solar zenith angles less than  $70^\circ$ , which is the range of incident angles for which the instrument cosine response errors are less than 7% (Figure 1). To remove variations in magnitude of the irradiance, all of the ratios were normalized at 490 nm.

The normalized spectral ratios were then grouped according to a cloud factor ( $CF$ ), the ratio of  $E_d(490)$  to  $\hat{E}_d(490)$ , and each group was then averaged (Figure 3). Low values of  $CF$  generally indicate large cloud volumes, whereas  $CF$  values of one indicate clear sky. Note that values for  $CF$  in the range 1.0–1.2 may be caused by reflection from the sides of clouds [Nack and Green, 1974; Segal and Davis, 1992; Mims and Frederick, 1994], or it may be an indication of discrepancies between model estimates and measurements at 490 nm (see Figure 2). The principal result from Figure 3 is that

the spectra of average ratios tilt with decreasing  $CF$ , increasing the ratios for shorter tilt wavelengths (within the 95% level of confidence). The case with the lowest values of  $CF$  yields values differing from the clear-sky case by up to almost 25% in the visible, when normalized at 490 nm. Further grouping according to solar zenith angle showed no discernable trends, indicating that the effects of changes in solar zenith angle on the spectral cloud effect were minimal for these conditions.

The deviation of the clear-sky case from a flat line may be a consequence of either instrumental effects and/or inaccurate modeling [ $X(\lambda)$ ]. To remove this effect, each average ratio in Figure 3 (as well as those not shown) is simply divided by the clear-sky ratio (the ratio for cloud factors of 1–1.2) in the same figure. This yields a new set of ratios representing the spectral effect that different cloud factors can have on irradiance, with first-order discrepancies between the model and measurements removed (Figure 4). In this analysis, the clear-sky case is now spectrally neutral, and the ratios show the same trends observed in Figure 3; the spectral shape of the cloud effect tilts with decreasing cloud factor. Note that this technique of dividing each average ratio by the clear-sky ratio removes effects such as the use of an inaccurate ground albedo or air mass type in the model, so that it reveals only those spectral effects that are compounded by the presence of clouds.

The spectral cloud effect [ $SCE(\lambda, CF)$ ] can be parameterized as a function of the cloud factor ( $CF$ ), by

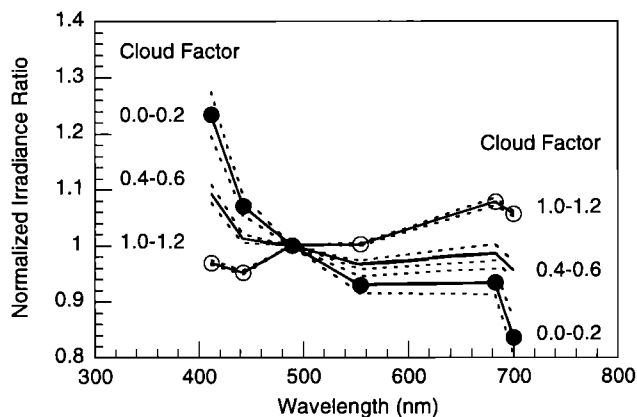


**Figure 3.** The effect of changes in the cloud factor (the ratio of measured to modeled irradiance at 490 nm) on the normalized irradiance ratio. The irradiance ratios shown are averages of the measured to modeled spectral irradiance ratios for each cloud factor group, normalized at 490 nm. The solid lines shown are for cloud factors in the ranges indicated for all cloud covers. The dotted lines are the 95% confidence intervals of the mean. The number of spectra averaged in each case shown were 36 ( $CF=0.0-0.2$ ; minimum observed was 0.043), 51 ( $CF=0.4-0.6$ ), and 102 ( $CF=1.0-1.2$ ). The number of spectra in the remaining cloud factor intervals (not shown) were 58 (0.2–0.4), 42 (0.6–0.8), and 78 (0.8–1.0).

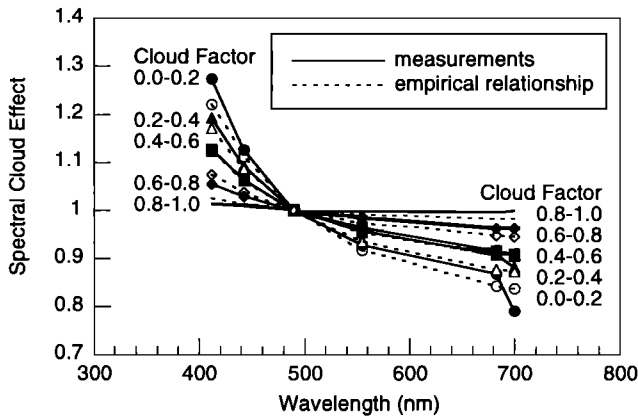


**Figure 4.** The spectral effect of different cloud factors on solar irradiance. Each solid line with solid symbols is the ratio of each solid line in Figure 3 (and those not shown) to the solid line in the same figure for cloud factors of 1.0-1.2 (i.e., approximately clear sky). This calculation removes the spectral effects caused by inaccuracies in the model results and by instrumental effects. The dotted lines with open symbols show the empirical spectral cloud effect (5) as a function of cloud factor for values of  $CF$  of 0.1, 0.3, 0.5, 0.7, and 0.9. The symbol shapes for the empirical lines are the same as the symbol shapes for the corresponding measured lines. All lines are normalized at 490 nm.

fitting power functions to the solid lines in Figure 4 of the form:

$$SCE(\lambda, CF) = a(CF) + b(CF)(\lambda/490)^{-n}, \quad (2)$$

where  $a(CF)$  and  $b(CF)$  are parameters that are functions of  $CF$  and  $n$  is the shape parameter. The relationships are confined by two restrictions: (1)  $SCE$  must equal 1 for all wavelengths when  $CF = 1$  and (2)  $SCE$  must equal 1 for all values of  $CF$  at a wavelength of 490 nm. Since the second restriction means that  $a(CF) + b(CF) = 1$ , (2) can be reduced to a function of two parameters:

$$SCE(\lambda, CF) = 1 - b(CF) + b(CF)(\lambda/490)^{-n}. \quad (3)$$

Fitting the data and applying the restrictions yielded the following linear relationship for  $b(CF)$ :

$$b(CF) = 0.24(1 - CF) \quad (4)$$

with a coefficient of correlation of greater than 0.99. The value of  $n$  that gave the best fit to the data was  $4 \pm 1$ . Cloud factors of greater than one were approximated by cloud factors of one for this analysis. Combining (3) and (4) with the best fit value for  $n$  yields

$$SCE(\lambda, CF) = 0.76 + 0.24CF + 0.24(1 - CF)(\lambda/490)^{-4} \quad (5)$$

for  $CF \leq 1$ , where  $\lambda$  is in units of nanometers. This empirical relationship is shown by the dotted lines in Figure 4 for cloud factors of 0.1, 0.3, 0.5, 0.7, and 0.9.

Comparison of the data to the empirical relationship shows the worst fit at long wavelengths, possibly because of the increased contribution from absorption by water near 695 nm. Refitting the data to the same type of power law after removing the data points at 700 nm yielded the same parameters within standard error. This type of function was found to fit the data better than previously derived linear functions of wavelength [Siegel *et al.*, 1998] and exponential fits.

## 7. The Fraction of Cloud Cover

In some cases, local measurements of the cloud factor may be unavailable, such as in remote locations or for studies over large spatial areas. A more convenient and readily available parameter for describing the amount of cloud cover in such cases is  $f$ , the fraction of cloud cover. Observations of  $f$  are routinely made at most weather stations and can also be made by eye on site or remotely using a camera. For larger spatial scales, estimates of  $f$  can be made from satellite measurements of cloud cover. Using a relationship between  $CF$  and  $f$ , it would be possible to parameterize  $SCE(\lambda, CF)$  as a function of  $f$ .

A number of previous studies [e.g., Kaiser and Hill, 1976; Kasten and Czeplak, 1980; Frederick and Steele, 1995; Davis, 1996] have derived relationships between the ratio of integrated cloudy irradiance ( $E_{\text{cloudy}}$ ) to integrated clear-sky irradiance ( $E_{\text{clear}}$ ) measured over large bandwidths (e.g., 300-2800 nm [Davis, 1996]) and the fraction of sky covered by either total cloud or opaque cloud (for a more comprehensive citation list see Kasten and Czeplak [1980]). For the purpose of this study,  $f$  will be assumed to be equivalent to the fraction of sky covered by opaque cloud (as given by Davis [1996]) rather than total cloud. The derived relationships varied in form from linear [Frederick and Steele, 1995] to power functions [Kaiser and Hill, 1976; Kasten and Czeplak, 1980; Davis, 1996] of  $f$ :

$$E_{\text{cloudy}}/E_{\text{clear}} = 1 - \alpha f^\beta, \quad (6)$$

where  $\alpha$  and  $\beta$  are parameters. These relationships implicitly include the effects of cloud thickness and solar zenith angle. A study covering 41 locations within Canada [Coombes and Harrison, 1987] yielded relationships of similar shape to the nonlinear forms found for Hamburg, Germany [Kasten and Czeplak, 1980] and Seattle, Washington [Davis, 1996] (equation (6)).

If it is assumed that the spectral effect of clouds will have a minimal second-order effect on the magnitude of  $E_{\text{cloudy}}$  (see section 11.2 for a discussion of the effect on PAR), the ratio  $E_{\text{cloudy}}/E_{\text{clear}}$  can be approximated by  $CF$ , which is based on irradiance ratios at 490 nm. A test of this assumption was made on data from Analytical Spectral Devices, Inc., who made measurements of spectral irradiance at 1 nm resolution from 350 to 2200 nm on successive clear and cloudy days (A. F. H. Goetz, Analytical Spectral Devices, Inc., personal communi-

cation, 1997). The ratio of cloudy to clear integrated irradiance (0.3103) was found to deviate from the ratio of cloudy to clear irradiance at 490 nm (0.3237) by 4%. Hence, assuming that  $E_{\text{cloudy}}/E_{\text{clear}}$  can be approximated by  $CF$  and that the empirical relationship derived by *Davis* [1996] for Seattle, Washington (equation (6),  $\alpha = 0.674$  and  $\beta = 2.854$ ), is applicable to Halifax, (5) can be expressed as a function of  $f$ :

$$SCE(\lambda, f) = 1 + 0.16f^{2.854}[(\lambda/490)^{-4} - 1], \quad (7)$$

where  $\lambda$  is in units of nanometers.

The irradiance ratios  $E_d(\lambda)/\hat{E}_d(\lambda)$  were divided into four groups according to the fraction of cloud cover (clear sky, scattered cloud (less than 1/2 sky covered), broken cloud (greater than 1/2 sky covered), and overcast) after normalizing at 490 nm and then averaged to determine the accuracy of this parameterization. These sky conditions were provided by Environment Canada at Shearwater on an hourly basis. Data from periods when sky conditions were designated as obscured (such as by dust) or raining were excluded. Instrumental and model deficiencies [ $X(\lambda)$ ] were removed by dividing the average ratio for each group by the average ratio for the clear-sky group (as in Figure 4). The comparison between the spectral cloud effect determined as a function of cloud cover and measurements showed good correspondence (Figure 5). The excellent agreement between the derived empirical relationship and the measured spectral effect of clouds indicates that the relationship between  $f$  and  $CF$  derived from *Davis* [1996] is appropriate for this data set.

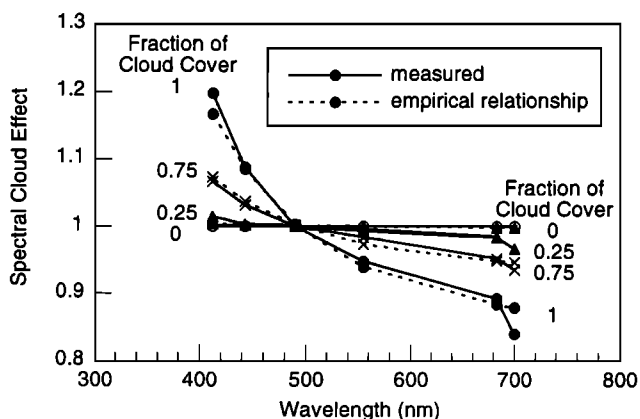


**Figure 5.** A comparison between the spectral effect of clouds determined here (solid lines) with the empirical relationship of (7) (dashed lines) for the four sky conditions (clear sky (open circles), scattered cloud (triangles), broken cloud (crosses), and overcast (solid circles)). The chosen values of  $f$  used in the empirical relationship of (7) for each sky condition were 0, 0.25, 0.75, and 1, respectively. Note that the two relationships for clear sky ( $f = 0$ ) are superimposed along a straight line.

## 8. Comparison with Previous Results

Previous studies have examined the spectral effects of clouds on downwelling irradiance in the visible [*Nann and Riordan*, 1991; *Byfield et al.*, 1997; *Siegel et al.*, 1998]. *Nann and Riordan* [1991] derived empirical relationships for the spectral effects based on measurements made in Germany and at three locations across the United States, compared with a clear-sky model. The fitted parameters for their nonlinear functions of wavelength were not published, so their results cannot be compared quantitatively with ours. However, their spectral cloud effects do show a nonlinear wavelength dependence in the visible similar to those presented here [*Nann and Riordan*, 1991, Figures 4b and 8]. *Siegel et al.* [1998] performed a similar analysis in the western equatorial Pacific Ocean for 13 wavebands between 340 and 683 nm and found linear relationships between the spectral cloud effect and wavelength. Their derived empirical relationships are given below:

$$cl(\lambda, CL) = A(CL)\lambda + B(CL), \quad (8)$$

where

$$A(CL) = 0.0015CL(1 - CL), \quad (9)$$

$$B(CL) = 0.966(CL)^2 + 0.0619CL - 0.0389, \quad (10)$$

and  $CL$  is defined as  $1 - (E_{\text{cloudy}}/E_{\text{clear}})$ . Note that  $CL$  is directly equivalent to  $0.674f^{2.854}$  based on the relationship by *Davis* [1996] (equation (6)) and approximately equal to  $1 - CF$ . The variable  $cl(\lambda, CL)$  is their spectral cloud index, which describes the combined spectral and magnitude effect of clouds on the downwelling irradiance. A cloudy spectrum can be obtained from  $cl(\lambda, CL)$  by multiplying the clear-sky spectrum by  $[1 - cl(\lambda, CL)]$ . The magnitude effect of clouds is removed from  $[1 - cl(\lambda, CL)]$  by normalizing at 490 nm.

A comparison of model fits shows that the two types of relationships show marked differences, particularly at shorter wavelengths (Figure 6). For example, our relationship yields a factor of 1.17 at 412 nm for overcast skies whereas the *Siegel et al.* [1998] relationship yields 1.07 under the same conditions. The difference between the two relationships may be a consequence of the assumption made for the comparison that  $E_{\text{cloudy}}/E_{\text{clear}} = CF$  (although it was demonstrated in section 7 that they differ by only 4%), or to different cloud types and aerosols present at the two locations under comparison, or to different ground albedos. In the same study, *Siegel et al.* [1998] found that the ratio of irradiance from a plane-parallel cloud radiative transfer model (SBDART) for cloudy sky to that for clear sky followed a nonlinear shape in the visible.

Analytical Spectral Devices, Inc., estimated the spectral cloud effect by taking the ratio of cloudy irradiance data to clear-sky irradiance data from the next day measured using a spectroradiometer at 1 nm resolution

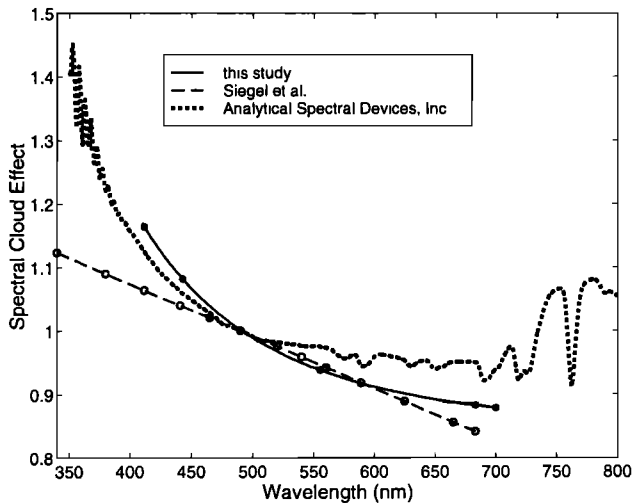


**Figure 6.** A comparison between two empirical relationships and an independent observation of the spectral cloud effect. The empirical relationships shown are that presented here (equation (5), solid line) and that derived by Siegel *et al.* [1998] (equations (8)-(10), dashed line), for a cloud factor of 0.33. Each empirical relationship is shown only over the wavelength region from which it was derived. The dotted line shows the normalized ratio of two irradiance measurements made by Analytical Spectral Devices, Inc., using a spectroradiometer at 1 nm resolution (data reproduced with permission). The measurements were made at approximately the same solar zenith angles on adjacent clear and cloudy days in April 1996 near the border of Oklahoma and Kansas. The value of  $CF$  for their measurements was 0.32. The fluctuations observed in their ratio below 400 nm may have been caused by calibration problems (A. F. H. Goetz, Analytical Spectral Devices, Inc., personal communication, 1997). The symbols on the Siegel *et al.* line and on the line from this study indicate the center wavelengths for which measurements were made.

(near the border of Oklahoma and Kansas) (A. F. H. Goetz, Analytical Spectral Devices, Inc., personal communication, 1997) (Figure 6). Note that the spectral cloud effect derived in this way also includes spectral effects caused by temporal variability of the local climatological parameters. The ratio of cloudy to clear-sky irradiance at 490 nm for this measurement (equivalent to  $CF$ ) was 0.32. This result also clearly shows the non-linear nature of the spectral effect of clouds, although it differs in shape from the spectral effect found for Halifax at the same value of  $CF$ . The high-resolution measurements by Analytical Spectral Devices, Inc., show little deviation from a smooth function, for wavelengths shorter than 700 nm. This indicates that although the empirical relationship presented here was based on data from only 6 wavebands in the visible wavelength region, it may provide estimates for the spectral effect of clouds to within 5% in the intervening wavelength regions. It also appears that the relationships presented here may

be valid for wavelengths as short as 350 nm and perhaps even 320 nm [see Webb, 1991, Table 1; Wang and Lenoble, 1996; Siegel *et al.*, 1998], although more studies need to be made in this wavelength region to confirm this. Extrapolation beyond 700 nm is not possible since the spectral cloud effect shows strong variability at these wavelengths (Figure 6). This is likely caused by the presence of water absorption bands at these wavelengths.

## 9. A Practical Test

Measurements of downwelling irradiance were made using the same OCI-200 irradiance meter in the Bering Sea (near 57°N, 168°W) aboard the R/V *Miller Freeman* from April 17-27, 1996. Downwelling irradiance was measured 6 times per second and averaged over 10-min periods for solar zenith angles less than 70°. Clear-sky model irradiances were calculated from the BRGC model using climatological parameters measured aboard the R/V *Miller Freeman* and corrected for the spectral response of the instrument. The climate data were available only every 3 hours, which resulted in only 14 comparable spectra. All spectra were normalized at 490 nm.

The instrumental and model effects were evaluated by dividing the irradiance measured during a period with less than 1/8 cloud cover by the corresponding clear-sky model irradiance. Note that no clear-sky data were available for this calculation from the subset of 14 spectra used. Each of the measured spectra were then divided by this correction spectrum. Figure 7a shows two comparisons of the spectral shape of the corrected irradiance measurements on a cloudy day with the clear-sky model. It can be seen that the spectral shapes differ; the measurements show relatively weaker attenuation at shorter wavelengths and stronger attenuation at longer wavelengths than the irradiances from the clear-sky model. This is similar to the effect seen in Halifax under cloudy conditions (Figure 5).

To test the applicability of the parameterization developed for Halifax to the data from the Bering Sea, the clear-sky model irradiances were multiplied by the estimated spectral cloud effects derived for Halifax, and the resulting irradiances were then compared with the Bering Sea measurements (Figure 7b). The irradiances are now closer in shape.

The agreement between the modeled irradiances and the instrument-corrected measured irradiances can be evaluated by studying the mean percentage difference (MPD). This is calculated at each wavelength in the following manner:

$$\text{MPD}(\lambda) = \frac{100}{N} \times \sum [E_i(\lambda) - \hat{E}_d(\lambda)]/E_i(\lambda), \quad (11)$$

where  $E_i(\lambda)$  is the instrument-corrected measured irradiance and  $N$  is the number of pairs of spectra. An MPD equal to zero indicates no bias, whereas posi-

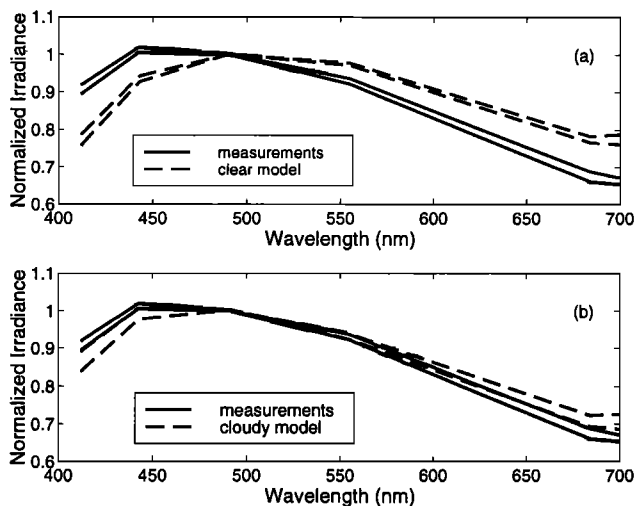


**Figure 7.** Comparison of irradiance spectra measured in the Bering Sea for two cloudy periods (solid lines) with (a) clear-sky model irradiances (dashed lines) and (b) cloudy model irradiances using the spectral cloud effect derived for Halifax (dashed lines). The modeled irradiances were corrected for the spectral response of the instrument, and the measurements were averaged over 10-min periods. Each of the averaged, measured spectra were divided by a correction spectrum to remove remaining instrumental effects and model artifacts. Each of the spectra has been normalized at 490 nm.

tive and negative MPDs indicate negative and positive model biases, respectively. The MPDs for the clear-sky model and the cloudy model are shown in Figure 8. The clear-sky model shows a negative bias (positive MPD) at short wavelengths and a positive bias (negative MPD) at long wavelengths, reaching magnitudes of up to 10%. The steady change in bias with wavelength is an indication of the spectral effect of clouds. The bias between the cloudy model presented here (derived for use in Halifax) and the Bering Sea data shows a similar spectral shape; however, its magnitude is almost halved. This shows that while the incorporation of the spectral effect of clouds improved the agreement between the measurements and the model, the spectral cloud effect determined in Halifax does not fully explain the irradiance changes observed in the Bering Sea. Also shown in Figure 8 are the MPDs found if the linear spectral cloud effect of Siegel *et al.* [1998] is used to model the Bering Sea data. The spectral effect of clouds appears to be a steeper function of wavelength in the Bering Sea than in Halifax or the western equatorial Pacific Ocean. This may be a result of the presence of different types of clouds in these locations, or it may be due to differences in ground albedo (see section 10). Because of the limited number of sets of climatological observations available (14), a spectral cloud effect could not be determined with statistical significance for the Bering Sea. Local studies of the spectral effects of clouds should be made if accurate spectral irradiances are required.

## 10. The Roles of Sky Reflectivity and Surface Albedo

Two causes for the spectral effect of clouds were introduced earlier: (1) reflection from the surface of the clouds and the ground and (2) spectral absorption and scattering by cloud particles and intervening gas molecules. The former effect is expected to be the dominant process [Middleton, 1954]; hence it may be possible to mimic the spectral effect of clouds by using existing clear-sky models and increasing the sky reflectivity within them. This is similar to the approach taken by Gardiner [1987], who derived a (nonspectral) model that accounts for the transmission and absorption of the cloud and multiple scattering between (1) the clouds and ground, (2) the clouds and sky, and (3) the sky and ground. Using this model, he showed that under cloudy skies in Antarctica, deviations in the magnitude of downwelling irradiance can be explained by deviations in the magnitude of ground albedo. This effect has also been seen in other studies in polar regions, where the ground albedo is extremely high [Ricchiuzzi *et al.*, 1995]. This observation has also been used to simulate increased irradiance under cloudy skies in a model by altering the magnitude of the ground albedo [Kylling *et al.*, 1997] and the sky reflectivity [Atwater and Ball, 1978]. Using a similar approach, sensitivity analyses are made here of the effects of the magnitude of the sky reflectivity and the magnitude and spectral shape of the surface albedo on spectral downwelling irradiance in regions of relatively low ground albedo (0.02-0.26) using the BRGC model.

The sky reflectivity [ $r_s(\lambda)$ ] is a function of all of the climatological parameters input in the BRGC model [see Bird and Riordan, 1986]. The BRGC model uses

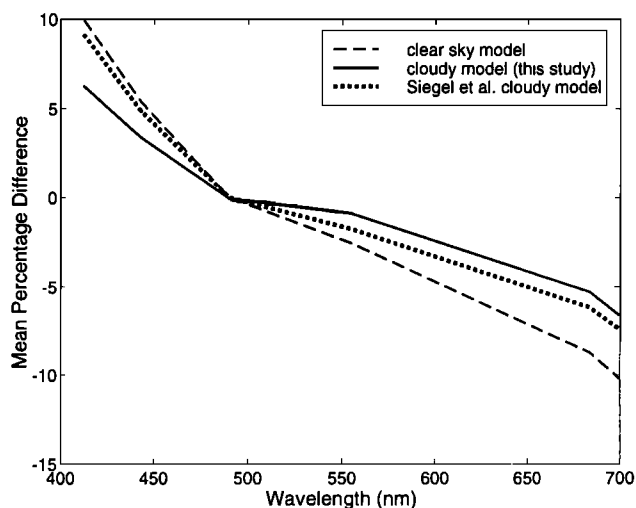


**Figure 8.** Mean percentage difference between modeled irradiance and instrument-corrected irradiance (equation (11)) measured in the Bering Sea as a function of wavelength for the clear-sky model (dashed line), the cloudy model derived here (solid line) and the Siegel *et al.* [1998] cloudy model (dotted line).

**Table 1.** Climatological Variables Used in the BRGC Model to Study the Effects of Variations in Sky Reflectivity and Ground Albedo on Downwelling Irradiance and the Effects of Clouds on Estimates of Biological Properties in the Ocean.

Variable	Value
Day of year	150
Longitude	63°W
Latitude	45°N
Solar zenith angle	30°
Pressure	1013 mbar
Relative humidity	70%
Water vapor concentration	4 cm <sup>-1</sup>
Visibility	30 km
Windspeed	2.6 m s <sup>-1</sup>
Mean 24-hour windspeed	2.6 m s <sup>-1</sup>
Ozone	300 DU
Air mass type	2
Surface type	land

These are typical values for Halifax, Nova Scotia.

the product of  $r_s(\lambda)$  and the ground albedo [ $r_g(\lambda)$ ] to derive the downwelling irradiance resulting from multiple air-ground interactions. Note that these two quantities are not independent; changes in the fraction of diffuse to direct irradiance caused by clouds can change the magnitude of the ground albedo [see *Bukata et al.*, 1995].

First, assuming a spectrally neutral ground albedo, clear-sky downwelling irradiance was calculated for increasing magnitudes of  $r_s(\lambda)$  using the climatological variables in Table 1. The magnitude of  $r_s(\lambda)$  was increased uniformly over all wavelengths by up to 6 times its clear-sky magnitude. This has the same effect on calculations of irradiance as increasing the magnitude of the ground albedo. A typical value for  $r_s(\lambda)$  under clear sky [ $r_{sc}(\lambda)$ ] at the wavelength of maximum sky reflectivity, 350 nm, is 0.35. Since the product  $r_s(\lambda)r_g(\lambda)$  under cloudy sky conditions must be less than 1, the value that this product can be increased by is limited to less than 14 for a ground albedo of 0.2 ( $14 \times 0.35 \times 0.2 = 1$ ).

Ratios of each of the resulting irradiance spectra to the irradiance spectrum for sky reflectivity under clear sky were then calculated (Figure 9). Figure 9 shows a close resemblance in the visible to the spectral cloud effect derived here (Figure 4) and to that derived from the SBDART cloudy model by *Siegel et al.* [1998] at all wavelengths shown. The fluctuations in the spectral shape near 553, 590, 650, and 700 nm correspond to similar fluctuations found in the Analytical Spectral Devices, Inc., ratio which was based solely on measurements (Figure 6). The change in the spectral shape near 330 nm has also been seen in some previous studies [Webb, 1991, Table 1; Wang and Lenoble, 1996; Siegel et al., 1998]. However, note that this effect was not observed in measurements made by *Seckmeyer et al.* [1996, Figure 3]; this may have resulted from the ozone

correction factor that they used which may have overcorrected their results.

Spectral variations in the downwelling irradiance measured at the ground result not only from ground-cloud reflections but also from cloud-sky reflections [Kylling et al., 1997]. Assuming that reflection from the cloud top is spectrally neutral, Figure 9 also represents the effect of increasing cloud-top albedo on downwelling irradiance. These results are consistent with the hypothesis that the spectral effect of clouds may be almost entirely a consequence of reflection from the cloud surface and ground, rather than from spectral variations caused by the passage of irradiance through cloud. It also yields the potential for direct incorporation of the spectral effect of clouds into clear-sky models.

A relationship between  $CF$  and the magnitude of the multiplication factor for the sky reflectivity used, [ $r_s(\lambda)/r_{sc}(\lambda)$ ], was derived by finding the best fit of the irradiance ratios (Figure 9) to the spectral cloud effect for Halifax (Figure 4), assuming a relationship for  $r_s(\lambda)$  of the form:

$$r_s(\lambda) = r_{sc}(\lambda)[1 + c(1 - CF)], \quad (12)$$

where  $c$  is a parameter. The best-fit value for  $c$  for the Halifax data using a ground albedo of 0.2 was  $8 \pm 2$ . A comparison of the irradiance ratios derived using this value for  $c$  with the spectral cloud effect measured in Halifax for six ranges of  $CF$  is shown in Figure 10. This method shows reasonable ability to predict the spectral effect of clouds provided that a local parameterization for the relationship between  $r_s(\lambda)$  and  $CF$  is known. Since the above relationship is an empirical one,

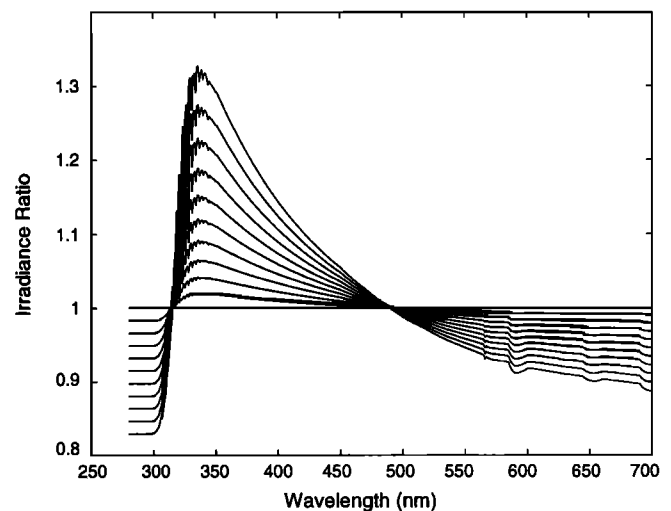


**Figure 9.** Variations in the ratio of clear-sky downwelling irradiance with enhanced sky reflectivities to that with normal sky reflectivity as a function of wavelength. The sky reflectivities were increased by factors of 1 to 6 using steps of 0.5. The irradiances were calculated using the BRGC model with the climatological parameters in Table 1 and a spectrally neutral ground albedo of 0.2. The sharp decrease in the irradiance ratio below 320 nm is caused by ozone absorption.

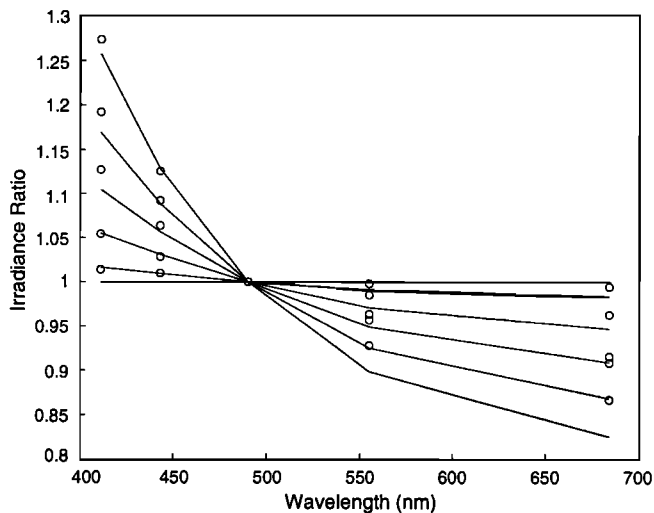


**Figure 10.** Comparison between the spectral cloud effect measured in Halifax at five wavebands (circles) with that estimated by changing the magnitude of the sky reflectivity in the BRGC model (lines). The measurements shown are for values of  $CF$  in ranges of 0.0-0.2, ..., 0.8-1.0. The lines were calculated using a derived empirical relationship for  $r_s(\lambda)$  in the BRGC model (equation (12)) for values of  $CF$  of 0.1, 0.3, ..., 0.9, and 1.0. Each line is the ratio of the downwelling irradiance for each value of  $CF$  to that for clear sky ( $CF = 1$ ). Only five wavebands were compared; the sixth at 699.5 nm showed poor agreement with the model results and hence was not used in the derivation of (12).

it implicitly incorporates the effects of multiple scattering between the ground, clouds, and sky (for a model that incorporates these effects explicitly, see *Gardiner* [1987]).

A sensitivity analysis of the effect of spectral variations in the ground albedo was performed by using the spectral albedo for concrete and its mirror image (Figure 11). The ground albedo of concrete was chosen as it may be representative of the Halifax region and because it has a relatively simple shape in the visible region; it increases almost linearly with increasing wavelength. Note that the mirror image has a similar spectral shape to the albedo (or irradiance reflectance) of open ocean water but differs in magnitude by a factor of approximately 10.

Using the spectral albedo for concrete, the irradiance ratio was recalculated using the empirical relationship of (12) for a value for  $CF$  of 0.1. In comparison to the case assuming a spectrally neutral ground albedo of 0.2 (Figure 12), the ratio for the spectral albedo of concrete shows less variation with changes in  $CF$ , in spite of the increased albedo (mean of 0.26). This raises two points: first that relationships derived for  $r_s(\lambda)$  as functions of  $CF$  depend on the chosen ground albedo and second that a ground albedo that increases with wavelength in the visible region tends to counteract the effects of increasing sky reflectivity. The opposite effect is seen when the mirror image of the spectral albedo of concrete

(Figure 11) is used (Figure 12). This spectral shape for ground albedo enhances the effect of increased sky reflectivity. However, the magnitude of the ground albedo is also important, as demonstrated using the spectral albedo of open ocean water whose magnitude is significantly lower than that of concrete (with a mean of 0.02). For this sensitivity analysis, the BRGC model was run using a ground type of land. When the appropriate ground type of water is used in the BRGC model, the deviation in the irradiance ratio from a clear-sky case is even less. The discrepancy observed between data from the Bering Sea, data from the equatorial Pacific and the spectral cloud effect derived for Halifax (Figure 8) may be caused by the difference in surface albedo between locations. Hence knowledge of the spectral shape and magnitude of the ground albedo is essential for accurate modeling of the spectral effect of clouds (using this method) as well as downwelling irradiance. Note that the method presented in section 6 to derive the spectral cloud effect for Halifax did not depend on an accurate choice for the ground albedo because of the correction ratio used.

In the approach presented here, we replaced the clear-sky reflectivity [ $r_{sc}(\lambda)$ ] in a clear-sky model with a surrogate sky reflectivity [ $r_s(\lambda)$ ], which is a linear function of  $r_{sc}(\lambda)$  and the cloud factor ( $CF$ ). Our results demonstrate that by using this approach, clear-sky models can be used to yield the spectral shape of downwelling irradiance in the presence of clouds. However, when the magnitude of the sky reflectivity in a clear-sky model is increased, the magnitude of the calculated downwelling irradiance also increases. To correct for this effect, the resulting "cloudy" irradiance must be normalized at 490

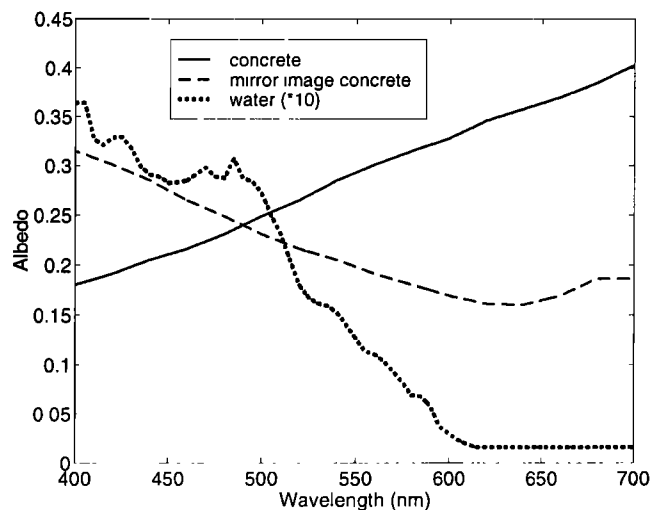


**Figure 11.** Spectral albedos for concrete (solid line) from *Gueymard* [1995], its mirror image about 490 nm (used for a sensitivity analysis) (dashed line), and for open ocean water near Cuba (see *Morel and Prieur* [1975], their Discoverer station 10) (dotted line). For the water albedo, a value of 0.00159 was assumed beyond 615 nm. Note that the water albedo has been multiplied by a factor of 10 in the figure.

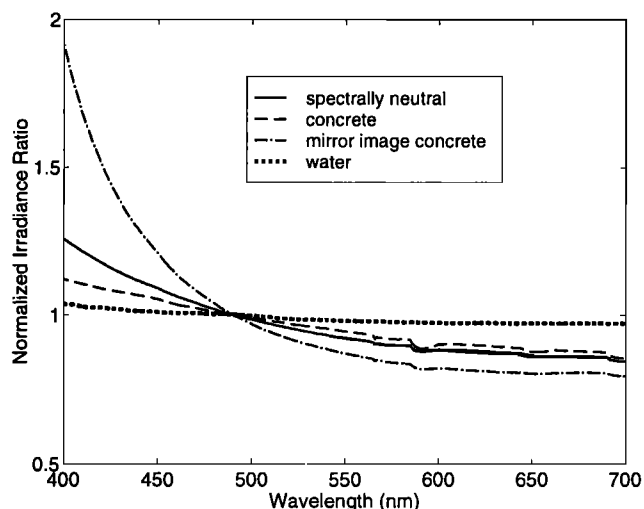


**Figure 12.** The effect of changes in the spectral shape and magnitude of the ground albedo on the ratio of irradiance under enhanced sky reflectivity to that under clear-sky reflectivity. In each case, the sky reflectivity was increased by a factor of 8.2, as determined by (12) for Halifax ( $c = 8$ ) under overcast conditions ( $CF = 0.1$ ). The ratio of the modeled irradiance under the enhanced sky reflectivity to that for clear-sky reflectivity ( $CF = 1$ ) is shown for four different ground albedos: a spectrally neutral surface with an albedo of 0.2 (solid line), concrete (dashed line), the mirror image of concrete about 490 nm (dotted-dashed line), and open ocean water (dotted line). Each of the irradiance ratios were normalized at 490 nm.

nm to either (1) the value of  $E_d(490)$ , if measured, or (2) the magnitude of the irradiance expected for clear-sky conditions at 490 nm, and subsequently corrected for cloud magnitude effects (e.g., (6)). This yields the magnitude and spectral shape of downwelling irradiance in the presence of clouds using a clear-sky model.

## 11. Biological Implications

In situ measurements of radiance and irradiance are often used to determine certain biological properties in the ocean, such as the concentration of chlorophyll  $a$ . Often these estimates are made without knowledge of spectral variations in the downwelling irradiance [Mueller, 1986; Cullen et al., 1994; Abbott and Letelier, 1997]. The effect of spectral variations in the downwelling irradiance, such as those caused by the presence of clouds, on the estimation of several biological properties and bio-optical properties at the sea surface is examined here. The properties studied include chlorophyll concentration as estimated from measurements of water-leaving radiance, PAR, and PUR.

### 11.1. Chlorophyll Concentration

The chlorophyll concentration at the sea surface is often estimated using empirical relationships between  $C$  and spectral ratios of reflectance at the sea surface,

$R(\lambda)$  [Morel, 1980], or ratios of water-leaving radiance at the sea surface,  $L_w(\lambda)$  [Gordon et al., 1983]. Since the ocean color is itself a function of the incident irradiance, knowledge of the spectral distribution of the downwelling irradiance is essential. The following analysis demonstrates the errors involved in estimates of  $C$  from in situ or aircraft measurements of  $L_w(\lambda)$  if spectral variations in the downwelling incident irradiance are ignored. One application of this analysis is the correction of measurements made by in situ moorings and drifters that are used to monitor variations in  $C$  under cloudy conditions when satellite measurements are not available. Note that this analysis may also apply to satellite measurements of ocean color, since clouds in neighboring pixels may affect the measurements from clear-sky pixels.

Water-leaving radiance can be converted to reflectance using the relationship

$$R(\lambda) = Q(\lambda)L_w(\lambda)/E_d(\lambda), \quad (13)$$

where  $Q(\lambda)$  is the ratio of upwelling irradiance to upwelling radiance. Assuming that the wavelength dependence of  $Q(\lambda)$  is negligible (but see Morel and Gentili [1993, 1996]), the ratio of reflectance [ $r_{ij} = R(\lambda_i)/R(\lambda_j)$ ] can be expressed as

$$r_{ij} = l_{ij}/e_{ij}, \quad (14)$$

where  $l_{ij}$  is the ratio of water-leaving radiances and  $e_{ij}$  is the ratio of downwelling irradiances. Combining a clear-sky irradiance spectrum, calculated using

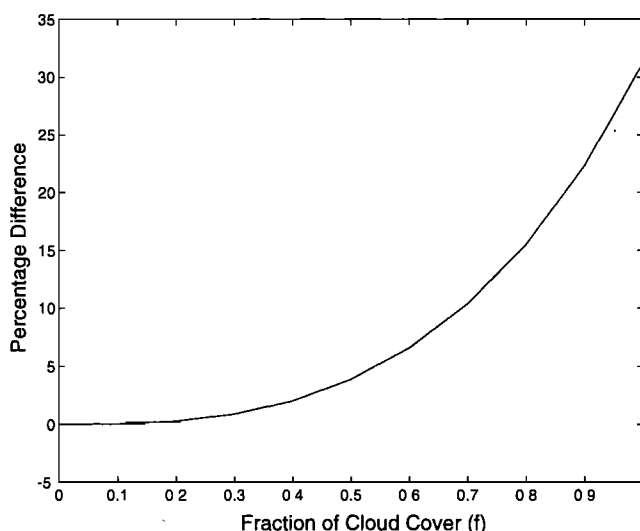


**Figure 13.** Percentage difference between  $C$  estimated assuming spectral cloud effects and  $C$  assuming a clear-sky spectral shape for the irradiance using the same radiance ratios as a function of the fraction of cloud cover. A positive percentage difference indicates that if the spectral cloud effect is ignored,  $C$  is underestimated. The algorithm used to estimate  $C$  was a function of the ratio of water-leaving radiances and the ratio of downwelling irradiances at 440 and 560 nm (see text).

the BRGC model with the parameters listed in Table 1 for an air mass type of 1 and an oceanic surface type, with the spectral effect of clouds (equation (7)), irradiance ratios for different cloud covers can be calculated and hence  $r_{\lambda}$  can be estimated for a range of radiance ratios. Using the reflectance ratio algorithm of Morel [1980] for open ocean (case 1) waters,  $C$  can then be estimated for these different sky conditions:

$$C = 1.92[R(440)/R(560)]^{-1.80}. \quad (15)$$

The percentage difference between  $C$  estimated incorporating the spectral effects of clouds and  $C$  estimated assuming a spectral shape for clear sky using the same radiance ratios is shown as a function of cloud cover in Figure 13. The percentage difference increases with increasing cloud cover up to over 30% for overcast conditions. In other words, if the spectral effects of clouds are ignored,  $C$  will be underestimated by up to 30% under cloudy skies using this algorithm. Hence the reflectance ratio is a strong function of the spectral shape of the downwelling irradiance. Note that the maximum percentage difference (in this case 30%) depends on the algorithm(s) used to estimate  $C$  and may vary as a function of  $C$  if different algorithms are used to describe different regions of the ocean. Also, note that the effect of clouds on estimates of  $C$  may be particularly significant during periods of scattered cloud, where the cloud effect can vary of the order of minutes depending on the location of the clouds in reference to the line-of-sight of the sun [Cullen *et al.*, 1994]. Algorithms that relate ratios of  $L_w(\lambda)$  to  $C$  directly [e.g., Gordon *et al.*, 1983] implicitly include the effects of spectral variations in the downwelling irradiance, and, for satellite imagery, the measurements are only made under clear skies (although neighboring pixels may be cloudy). Estimates of  $C$  from measurements of  $L_w(\lambda)$  at the sea surface and from aircraft and satellites may be improved by explicitly accounting for spectral variations in the downwelling irradiance caused by clouds.

### 11.2. PAR

Photosynthetically available radiation is the integrated irradiance over the wavelength range 400–700 nm, the range over which plants, such as phytoplankton, typically utilize absorbed light for photosynthesis. PAR is often used as a measure of irradiance available for photosynthesis. The spectral effect of clouds on PAR is examined here by using a general irradiance spectrum at the sea surface (using nominal input values in the BRGC model: Table 1 with an air mass type of 1 and an oceanic surface type) and altering the spectral shape using the empirical relationship derived here (equation (7)) for values of  $f$  from 0 to 1. PAR is calculated by integrating the irradiance, in units of  $\text{mol m}^{-2} \text{s}^{-1} \text{nm}^{-1}$ , for each value of  $f$  used. PAR calculated using spectral cloud effects was found to be less than that assuming no spectral effects by a maximum of 3.8% for overcast

skies. In other words, PAR can be estimated to within 3.8% of the actual value under all cloud conditions by assuming a clear-sky spectral shape for the irradiance. Hence, since the spectral effects of clouds on PAR at the sea surface are relatively small, they can in most cases be neglected.

### 11.3. PUR

Photosynthetically usable radiation describes the fraction of incident radiation that can be absorbed by phytoplankton. It is an integral component in models of primary production [e.g., Kiefer and Mitchell, 1983; Morel, 1991]. This factor is described by the following relationship [Morel, 1978, 1991]:

$$\text{PUR}(z) = \int_{400}^{700} E_o(\lambda, z) a'_{ph}^*(\lambda) d\lambda, \quad (16)$$

where  $E_o(\lambda, z)$  is the scalar irradiance at depth  $z$  and  $a'_{ph}^*(\lambda)$  is the specific absorption coefficient of phytoplankton normalized at the maximum value of absorption [from Hoeffner and Sathyendranath, 1993]. The coefficient  $a'_{ph}^*(\lambda)$  has a spectral shape that generally shows strong absorption over a broad wavelength region near 440 nm and a relatively weaker absorption peak over a smaller region near 670 nm.

The value of  $E_o(\lambda, z)$  was recalculated for different values of  $f$  at the sea surface, to determine the effect of spectral variations in the irradiance on  $\text{PUR}(0)$ . Estimates of  $\text{PUR}(0)$  were found to be underestimated by about 1% under overcast conditions when the spectral effects of clouds were neglected. Hence  $\text{PUR}(0)$  varies by less than 1% under changing cloud conditions.

## 12. Summary

Autumn clouds over Halifax, Nova Scotia, were found to attenuate the downwelling solar irradiance according to the relationship  $a(CF \text{ or } f) + b(CF \text{ or } f)(\lambda/490)^{-4}$  in the visible. This relationship differs from both the linear relationship found in the western equatorial Pacific Ocean [Siegel *et al.*, 1998] and the stronger spectral effect found for clouds in the Bering Sea. Hence the spectral effect of clouds appears to be site-dependent and may be a function of a combination between the cloud type (or color) and the ground albedo. It was shown that the spectral cloud effect can be mimicked by using a clear-sky irradiance model and varying the magnitude of the sky reflectivity. This effect was found to be a strong function of the magnitude and spectral shape of the ground albedo. Further study of the ability of this method to accurately represent the spectral effect of clouds in the ultraviolet and visible regions is necessary. Similar studies at a range of locations are also necessary before a general model describing the spectral effect of clouds (perhaps as a function of atmospheric type, season, and surface albedo) can be attempted. A general model would be of great benefit

to studies where local estimates of the spectral effect of clouds is impractical. One application of these results is improved accuracy in estimates of biological properties from in situ optical measurements, particularly those that use algorithms based on wavelength ratios.

## Appendix: The BRGC Model

Clear-sky irradiances were modeled in this study using a combination of the Bird and Riordan model [Bird and Riordan, 1986] and a modified form of this model by Gregg and Carder [1990]. The additions and changes made to these models are outlined briefly here.

Several extra equations were incorporated in the BRGC model to derive necessary parameters from available data. These included expressions to derive (1) the relative humidity from the pressure, temperature, and dewpoint temperature (based on Lowe [1977]) and (2) the water vapor concentration from dewpoint temperature [Atwater and Ball, 1976].

Slight modifications were made to some of the equations given by Gregg and Carder [1990]. These included (1) replacing the constant 118.3 by 118.93 in their equation for the transmittance due to oxygen absorption (their equation (18)), (2) removing the extra factor of 1/2 appearing within the brackets of their equation for Fresnel's law (their equation (44)), (3) adding an expression for multiple sea-air interactions based on the method used by Bird and Riordan [1986], and (4) incorporating the correction factor for scattered irradiance derived by Bird and Riordan [1986] (their equation (28)). The first of these modifications is based on close examination of Leckner's [1978] derivation of this equation, which appears to have a typographical error in the final result. The last two modifications were made in an attempt to increase the accuracy of the model, by accounting for two factors that were not included in the Gregg and Carder model.

The BRGC model was designed with an option for choosing calculations applicable to land or water surfaces. The water calculations followed the equations by Gregg and Carder [1990] (apart from the slight modifications outlined above). The land calculations were performed by calculating the following parameters using the relevant relationships from Bird and Riordan [1986]: (1) the single scattering albedo and (2) the influence of multiple ground-air interactions. A further difference between the ocean and land calculations is the air mass type input into the model.

## Notation

N-D indicates a dimensionless parameter.

$a(CF)$	parameter for $SCE(\lambda, CF)$ (N-D).
$a_{ph}^*(\lambda)$	normalized specific absorption coefficient of phytoplankton (N-D).
$A(CL)$	parameter for $cl(\lambda, CL)$ ( $\text{nm}^{-1}$ ).
$b(CF)$	parameter for $SCE(\lambda, CF)$ (N-D).

$B(CL)$	parameter for $cl(\lambda, CL)$ (N-D).
BRGC model	combined Bird and Riordan [1986] model with the Gregg and Carder [1990] model.
$c$	parameter in the equation for $r_s(\lambda)$ (N-D).
$cl(\lambda, CL)$	spectral cloud index (N-D).
$C$	chlorophyll concentration ( $\text{mg m}^{-3}$ ).
$CF$	cloud factor [ $E_d(490)/\hat{E}_d(490)$ ] (N-D).
$CL$	cloud index [ $1 - E_{\text{cloudy}}/E_{\text{clear}}$ ] (N-D).
$e_{ij}$	ratio of downwelling irradiances [ $E_d(\lambda_i)/E_d(\lambda_j)$ ] (N-D).
$E_{\text{clear}}$	(wide-band) clear-sky irradiance ( $\text{W m}^{-2}$ ).
$E_{\text{cloudy}}$	(wide-band) cloudy irradiance ( $\text{W m}^{-2}$ ).
$E_d(\lambda, f)$	measured downwelling irradiance under cloudy sky ( $\mu\text{W cm}^{-2} \text{nm}^{-1}$ ).
$E_d(\lambda)$	modeled downwelling irradiance ( $\mu\text{W cm}^{-2} \text{nm}^{-1}$ ).
$E_i(\lambda)$	normalized instrument-corrected measured irradiance (N-D).
$E_o(\lambda, z)$	scalar irradiance ( $\text{mol m}^{-2} \text{nm}^{-1} \text{s}^{-1}$ ).
$f$	fraction of sky covered by cloud (N-D).
$l_{ij}$	ratio of water-leaving radiances [ $L_w(\lambda_i)/L_w(\lambda_j)$ ] (N-D).
$L_w(\lambda)$	water-leaving radiance ( $\text{W m}^{-2} \text{nm}^{-1} \text{sr}^{-1}$ ).
$MPD(\lambda)$	mean percentage difference (%).
$n$	exponent for $SCE(\lambda, CF)$ (N-D).
$N$	number of pairs of spectra (N-D).
PAR	photosynthetically available radiation ( $\text{mol m}^{-2} \text{s}^{-1}$ ).
PUR( $z$ )	photosynthetically usable radiation ( $\text{mol m}^{-2} \text{s}^{-1}$ ).
$Q(\lambda)$	ratio of upwelling irradiance to upwelling radiance (sr).
$r_g(\lambda)$	ground albedo (N-D).
$r_{ij}$	ratio of reflectances [ $R(\lambda_i)/R(\lambda_j)$ ] (N-D).
$r_s(\lambda)$	sky reflectivity (N-D).
$r_{sc}(\lambda)$	sky reflectivity for clear sky (N-D).
$R(\lambda)$	irradiance reflectance (N-D).
$SCE(\lambda, CF)$	spectral cloud effect (N-D).
$X(\lambda)$	instrumental and/or local effect on irradiance measurements (N-D).
$z$	depth (m).
$\alpha$	parameter for $E_{\text{cloudy}}/E_{\text{clear}}$ (N-D).
$\beta$	parameter for $E_{\text{cloudy}}/E_{\text{clear}}$ (N-D).
$\lambda$	wavelength (nm).

**Acknowledgments.** We are very grateful to both Keith Freeman and Keith Keddy at Environment Canada for providing the climatological data on a regular basis. We are

indebted to Scott McLean, Chantall Arsenault, and Heike Wuenschmann at Satlantic, Inc., for their technical assistance with the instrument. Thanks also to Geoff MacIntyre and Ed Officia for their help with the instrumental set up, Qiang Fu, Valborg Byfield, and Sasha Madronich for helpful discussions on clouds, and Dave Siegel for providing us with a copy of his manuscript. We would also like to thank Marlon Lewis and Mark Abbott for providing general assistance, and Wade Blanchard for his statistical advice. We also thank Ricardo Letelier and two anonymous reviewers for their helpful comments on the manuscript. Support for this study was provided by grants from NSERC Research Partnerships, NOAA/FOCI, and ONR. AMC was also supported by CNPq, Brazil. This is CEOTR publication number 15.

## References

- Abbott, M. R., and R. M. Letelier, Bio-optical drifters: Scales of variability of chlorophyll and fluorescence, in *Ocean Optics XIII*, edited by S. Ackleson and R. Frouin, *Proc. SPIE Int. Soc. Opt. Eng.*, 2963, 216-221, 1997.
- Atwater, M. A., and J. T. Ball, Comparison of radiation computations using observed and estimated precipitable water, *J. Appl. Meteorol.*, 15, 1319-1320, 1976.
- Atwater, M. A., and J. T. Ball, A numerical solar radiation model based on standard meteorological observations, *Sol. Energy*, 21, 163-170, 1978.
- Bird, R. E., and C. Riordan, Simple solar spectral model for direct and diffuse irradiance on horizontal and tilted planes at the Earth's surface for cloudless atmospheres, *J. Clim. Appl. Meteorol.*, 25, 87-97, 1986.
- Bukata, R. P., J. H. Jerome, K. Y. Kondratyev, and D. V. Pozdnyakov, *Optical Properties and Remote Sensing of Inland and Coastal Waters*, 362 pp., CRC Press, Boca Raton, 1995.
- Byfield, V., J. Cook, and S. R. Boxall, Variation in incident light with time of day and cloud conditions at Hurst Spit, UK South Coast, in *Ocean Optics XIII*, edited by S. Ackleson and R. Frouin, *Proc. SPIE Int. Soc. Opt. Eng.*, 2963, 148-153, 1997.
- Coombes, C. A., and A. W. Harrison, Influence of solar elevation on estimates of cloud cover, *Atmos. Ocean*, 25, 82-101, 1987.
- Cullen, J. J., A. M. Ciotti, and M. R. Lewis, Observing biologically induced optical variability in coastal waters, in *Ocean Optics XII*, edited by J. S. Jaffe, *Proc. SPIE Int. Soc. Opt. Eng.*, 2258, 105-115, 1994.
- Davis, R. F., Comparison of modeled to observed global irradiance, *J. Appl. Meteorol.*, 35, 192-201, 1996.
- Frederick, J. E., The climatology of solar UV radiation at the Earth's surface, *Photochem. Photobiol.*, 65, 253-254, 1997.
- Frederick, J. E., and H. D. Steele, The transmission of sunlight through cloudy skies: An analysis based on standard meteorological information, *J. Appl. Meteorol.*, 34, 2755-2761, 1995.
- Gardiner, B. G., Solar radiation transmitted to the ground through cloud in relation to surface albedo, *J. Geophys. Res.*, 92, 4010-4018, 1987.
- Gordon, H. R., D. K. Clark, J. W. Brown, O. B. Brown, R. H. Evans, and W. W. Broenkow, Phytoplankton pigment concentrations in the Middle Atlantic Bight: Comparison of ship determinations and CZCS estimates, *Appl. Opt.*, 22, 20-36, 1983.
- Gregg, W. W., and K. L. Carder, A simple spectral solar irradiance model for cloudless maritime atmospheres, *Limnol. Oceanogr.*, 35, 1657-1675, 1990.
- Gueymard, C., *SMARTS2, A Simple Model of the Atmospheric Radiative Transfer of Sunshine, version 2.7*, Florida Solar Energy Center, Cape Canaveral, 1995.
- Hoepffner, N., and S. Sathyendranath, Determination of the major groups of phytoplankton pigments from the absorption spectra of total particulate matter, *J. Geophys. Res.*, 98, 22789-22803, 1993.
- Kaiser, J. A. C., and R. H. Hill, The influence of small cloud covers on the global irradiance at sea, *J. Geophys. Res.*, 81, 395-398, 1976.
- Kasten, F., and G. Czeplak, Solar and terrestrial radiation dependent on the amount and type of cloud, *Sol. Energy*, 24, 177-189, 1980.
- Kiefer, D. A., and B. G. Mitchell, A simple, steady state description of phytoplankton growth based on absorption cross section and quantum efficiency, *Limnol. Oceanogr.*, 28, 770-776, 1983.
- Kneizys, F. X., E. P. Shettle, W. O. Gallery, J. H. Chetwynd, L. W. Abreu, J. E. A. Selby, S. A. Clough, and R. W. Fenn, Atmospheric transmittance/radiance: Computer code LOWTRAN 6, *Rep. AFGL-TR-83-0187*, U. S. Air Force Geophysics Laboratory, Hanscom AFB, Bedford, Mass., 1983.
- Kylling, A., A. Albold, and G. Seckmeyer, Transmittance of a cloud is wavelength-dependent in the UV-range: Physical interpretation, *Geophys. Res. Lett.*, 24, 397-400, 1997.
- Leckner, B., The spectral distribution of solar radiation at the Earth's surface: Elements of a model, *Sol. Energy*, 20, 143-150, 1978.
- Lowe, P. R., An approximating polynomial for the computation of saturation vapor pressure, *J. Appl. Meteorol.*, 16, 100-103, 1977.
- Middleton, W. E. K., The color of the overcast sky, *J. Opt. Soc. Am.*, 44, 793-798, 1954.
- Mims, F. M., III, and J. E. Frederick, Cumulus clouds and UV-B, *Nature*, 371, 291, 1994.
- Morel, A., Available, usable, and stored radiant energy in relation to marine photosynthesis, *Deep Sea Res.*, 25, 673-688, 1978.
- Morel, A., In-water and remote measurements of ocean color, *Boundary Layer Meteorol.*, 18, 177-201, 1980.
- Morel, A., Light and marine photosynthesis: A spectral model with geochemical and climatological implications, *Prog. Oceanogr.*, 26, 263-306, 1991.
- Morel, A., and B. Gentili, Diffuse reflectance of oceanic waters, II, Bidirectional aspects, *Appl. Opt.*, 32, 6864-6879, 1993.
- Morel, A., and B. Gentili, Diffuse reflectance of oceanic waters, III, Implication of bidirectionality for the remote-sensing problem, *Appl. Opt.*, 35, 4850-4862, 1996.
- Morel, A., and L. Prieur, Analyse spectrale des coefficients d'attenuation diffuse, de reflexion diffuse, d'absorption et de retrodiffusion pour diverses regions marines: *Rep. No. 17*, Centre de Recherches Oceanographiques de Villefranche-sur-Mer, Villefranche-sur-Mer, France, 1975.
- Mueller, J. L., Multiple wavelength method for filtering cloud shadows from oceanic spectral irradiance profiles, in *Ocean Optics VIII*, edited by M. A. Blizard, *Proc. SPIE Int. Soc. Opt. Eng.*, 108-114, 1986.
- Nack, M. L., and A. E. S. Green, Influence of clouds, haze, and smog on the middle ultraviolet reaching the ground, *Appl. Opt.*, 13, 2405-2415, 1974.
- Nann, S., A cloud cover modifier for solar spectral irradiance modelling, paper presented at International Solar Energy Society Solar World Congress, Int. Solar Energy Soc., Kobe, Japan, 1990.
- Nann, S., and C. Riordan, Solar spectral irradiance under clear and cloudy skies: Measurements and a semiempirical model, *J. Appl. Meteorol.*, 30, 447-462, 1991.
- Platt, T., and S. Sathyendranath, Oceanic primary produc-

- tion: Estimation by remote sensing at local and regional scales, *Science*, *241*, 1613-1620, 1988.
- Ricchiuzzi, P., C. Gautier, and D. Lubin, Cloud scattering optical depth and local surface albedo in the Antarctic: Simultaneous retrieval using ground-based radiometry, *J. Geophys. Res.*, *100*, 21091-21104, 1995.
- Ricchiuzzi, P. J., S. Yang, C. Gautier, and D. Sowle, SB-DART: A research and teaching software tool for plane-parallel radiative transfer in the Earth's atmosphere, *Bull. Am. Meteorol. Soc.*, in press, 1998.
- Seckmeyer, G., R. Erb, and A. Albold, Transmittance of a cloud is wavelength-dependent in the UV-range, *Geophys. Res. Lett.*, *23*, 2753-2755, 1996.
- Segal, M., and J. Davis, The impact of deep cumulus reflection on the ground-level global irradiance, *J. Appl. Meteorol.*, *31*, 217-222, 1992.
- Sherry, J. E., and C. G. Justus, A simple hourly clear-sky solar radiation model based on meteorological parameters, *Sol. Energy*, *30*, 425-431, 1983.
- Siegel, D. A., T. K. Westberry, and J. C. Ohlmann, On cloud color and ocean radiant heating, *J. Chm.*, in press, 1998.
- Spinhirne, J. D., and A. E. S. Green, Calculation of the relative influence of cloud layers on received ultraviolet and integrated solar radiation, *Atmos. Environ.*, *12*, 2449-2454, 1978.
- Wang, P., and J. Lenoble, Influence of clouds on UV irradiance at ground level and backscattered exittance, *Adv. Atmos. Sci.*, *13*, 217-228, 1996.
- Webb, A. R., Solar ultraviolet radiation in Southeast England: The case for spectral measurements, *Photochem. Photobiol.*, *54*, 789-794, 1991.
- 
- J. S. Bartlett, College of Oceanic and Atmospheric Sciences, Oregon State University, 104 Ocean Admin. Bldg., Corvallis, OR 97331. (e-mail: jasmine@oce.orst.edu)
- A. M. Ciotti, J. J. Cullen, and R. F. Davis, Department of Oceanography, Dalhousie University, Halifax, Nova Scotia, B3H 4J1, Canada. (e-mail: aurea@raptor.ocean.dal.ca; John.Cullen@dal.ca; richard.davis@dal.ca)

(Received April 1, 1998; revised August 18, 1998; accepted August 31, 1998.)